

LETTERS TO THE EDITOR

ASTROPHYSICS

Rotational Period of the Planet Mercury

IN a recent communication by S. J. Peale and T. Gold¹ the rotational period of Mercury, determined from radar Doppler-spread measurements to be 59 ± 5 days², has been explained in terms of a solar tidal torque effect, taking into account the large eccentricity of Mercury's orbit, and the $1/r^6$ dependence of the tidal friction (r being the Sun-planet distance). They conclude from a very brief discussion that after slowing down from a higher direct angular velocity, the planet will have a final period of rotation between 56 and 88 days, depending on the assumed form of the dissipation function. However, from their discussion it is by no means clear why permanent deformations would imply a period of 88 days as a final rotation state after a slowing-down process. A very nearly uniform rotational motion of 58.65 sidereal-day period, that is $2/3$ of the orbital period, may indeed be a stable periodic solution. This rotational motion could have the axis of minimum moments of inertia nearly aligned with the Sun-Mercury radius vector at every perihelion passage. The orbital angular velocity at perihelion ($2\pi/56.6$ days) is close to $2\pi/58.65$ days, leading to an approximate alignment of the axis of minimum moment of inertia with the radius vector in an arc around perihelion where the interaction is strongest. The axial asymmetry of Mercury's inertia ellipsoid may result in a torque that counterbalances the tidal torque, giving a stable motion with this orientation and with a period two-thirds of the orbital period. It would therefore be possible for Mercury to have a higher permanent rigidity than that permitted by Peale and Gold.

In discussion with I. I. Shapiro³, we concluded that the actual rotational motion may have evolved via a speeding-up process from a lower angular velocity or possibly from a retrograde motion. We would point out that a 58.65-day period, precisely because it is $2/3$ of the orbital period, fits some of the old optical observations as well as the recent radar measurements.

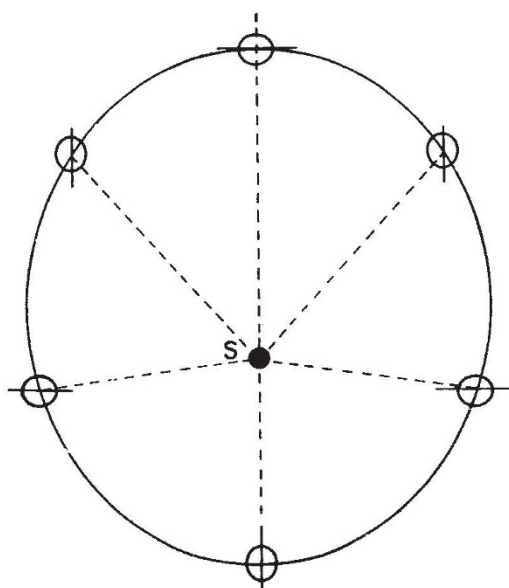


Fig. 1

In Fig. 1 a rough planar sketch is shown of the orientation of Mercury's axis of minimum moment of inertia, at different points along its orbit, given that the rotational period is two-thirds of the orbital period and that this axis is aligned with the Sun-planet vector at perihelion.

G. COLOMBO

University of Padova, Italy, and
Smithsonian Astrophysical Observatory,
Cambridge,
Massachusetts.

¹ Peale, S. J., and Gold, T., *Nature*, **206**, 1241 (1965).² Pettingill, G. H., and Dyce, R. B., *Nature*, **206**, 1240 (1965).³ Shapiro, I. I. (personal communication).

ASTRONOMY

Filamentary Nebulosity in the Vicinity of the Cetus Arc

FORMING large diameter circles across the sky are three ridges of enhanced radio emission. They are the North Polar Spur¹, 111° in diameter, the Cetus Arc², 91° diameter, and a third, unnamed, 60° diameter loop centred on the northern celestial pole³.

The radio continuum emission from these features is identical to that from the old supernova remnants. However, the nature of the 60° diameter loop is complicated by its correlation with twelve high-velocity neutral hydrogen clouds⁴. It has therefore been suggested that two, if not the third, of these objects are the remnants of nearby supernova explosions.

The principal difficulty to the acceptance of this theory has been the lack of detection of any optical emission regions coincident with these loops^{5,6}. All the accepted supernova remnants have characteristic filamentary nebulosity bounding their radio regions.

Such nebulosity has recently been searched for, on these three radio sources, in a photographic programme carried out at the high-altitude observatories of Jungfraujoch and Pic du Midi. Photographs were taken with small, high-speed camera and filter combinations which had low detection limits for emission nebulosity.

A further effective method of detecting faint, large-scale nebulosity was also used on this problem. In this, Palomar Sky Survey plates were copied at reduced scale and very high contrast. These were then compiled to form mosaics across the radio features. Faint density changes that were continuous through adjacent plates were considered to be caused by nebulosity.

The results produced by this work are as follows: (a) No filamentary nebulosity was detected on the North Polar Spur. However, a very diffuse optical emission region was shown to be present over this area. As yet it is impossible to say whether or not this is associated with the radio feature. (b) No filamentary nebulosity has been found on the 60° diameter loop. A search for diffuse nebulosity is now being undertaken. (c) It was on the Cetus Arc that the most interesting nebulosity was discovered. This has been sketched against the 237-Mc/s radio contours and presented in Fig. 1. The most striking single feature of this optical emission zone is the huge arc of nebulosity which bounds it. This is of filamentary micro-structure and has so far been traced for a length of 28° . Within this arc, towards the Cetus Arc radio ridge, there is a zone of diffuse elongated filaments. These merge with a structureless optical emission region as the radio